Acoustic emission from magnetic flux tubes in the solar network

Acoustic emission from magnetic flux tubes in the solar network

G Vigeesh[1] **and S S Hasan**[2]

[1] Department of Astronomy, New Mexico State University, Las Cruces, NM, U.S.A.
[2] Indian Institute of Astrophysics, Koramangala, Bangalore, India

E-mail: `vigeesh@nmsu.edu, hasan@iiap.res.in`

Abstract. We present the results of three-dimensional numerical simulations to investigate the excitation of waves in the magnetic network of the Sun due to footpoint motions of a magnetic flux tube. We consider motions that typically mimic granular buffeting and vortex flows and implement them as driving motions at the base of the flux tube. The driving motions generates various MHD modes within the flux tube and acoustic waves in the ambient medium. The response of the upper atmosphere to the underlying photospheric motion and the role of the flux tube in channeling the waves is investigated. We compute the acoustic energy flux in the various wave modes across different boundary layers defined by the plasma and magnetic field parameters and examine the observational implications for chromospheric and coronal heating.

1. Introduction

Observations of the solar surface in various filtergrams show a distribution of bright points, which are generally associated with an underlying concentrated magnetic field located in intergranular lanes [1]. Magnetic flux accumulates here after being swept in by granular flow forming strong vertical flux tubes at the junction of granules. The continually changing solar photosphere perturbs these magnetic structures resulting in the generation of magnetohydrodynamic (MHD) waves that propagate within the flux tube and also into the ambient plasma. The waves are excited by impulses imparted by granules. Eventually, the flux tubes are advected towards regions of stronger downdrafts present at the intersections of two or more granules where convectively driven vortex flows occur. The footpoints of the magnetic field structures are dragged in the vortex resulting in, presumably, a different source of wave excitation in the flux tube [2]. The conditions that prevail in the lower atmosphere impacts the upper layers, primarily through magnetic fields. Estimating the energy supplied by various photospheric disturbance will help us to determine the fraction of the overall heating of the upper atmosphere by wave sources. In order to examine energy transport to the outer layers of the quiet solar atmosphere mediated by magnetic fields [3–6], we need to clearly understand how the magnetic flux tube reacts to different types of perturbations. Despite being idealized representations of the actual processes, studies have shown that various wave-driven energy transport mechanisms are possible in a magnetized atmosphere [7–12]. Further investigations could reveal how these processes contribute to the overall energy budget and shed light on the significance of wave related sources. The purpose of this paper is to study two such scenarios with the aim of evaluating them in terms of their contribution to the heating of chromosphere and corona.

In this paper, we investigate the excitation of waves in magnetic flux tubes extending vertically through the solar atmosphere. This work is an extension of our previous study [12] that dealt with 3D modeling of MHD wave propagation in a magnetic flux tube embedded in a stratified atmosphere. We showed that there are possibly more than one mechanism of wave production effective which can lead to temporal variations of the emission that occur at chromospheric heights above these elements. In this paper our focus is to investigate the generations of acoustic waves excited by these perturbations and estimate the acoustic energy flux at different levels in the flux-tube. We calculate and compare the acoustic emission from various boundaries in the flux-tube and also from different β (the ratio of gas to magnetic pressure) surfaces as a result of the excitation.

2. Equilibrium Model and Boundary Conditions
Details of the equilibrium model that we consider in this study are given in [12]. Briefly, we consider an intense (kG field strength at the base) axially symmetric magnetic flux tube in a stratified solar model atmosphere that is in magnetostatic equilibrium. The temperature in the model increases with height to include the chromospheric temperature rise. The footpoint of the flux tube is located in the solar photosphere. The mathematical construction of the flux tube is described in the Appendix of [12] and the equilibrium properties of the flux tube are given in Table 1. The plasma-$\beta = 1$ surface essentially outlines the flux tube boundary in the lower part

Table 1. The equilibrium model parameters on the axis of the flux tube and ambient medium (values shown within brackets).

Height	T (K)	ρ (kg m^{-3})	P (N m^{-2})	c_S (km s^{-1})	v_A (km s^{-1})	B (G)	β
$z=1$ Mm	7263 (7195)	3.4×10^{-8} (1.0×10^{-7})	1.6 (4.8)	8.8 (8.7)	77.7 (39.2)	161 (141)	64 (16)
$z=0$ Mm	4768 (4766)	1.3×10^{-4} (4.0×10^{-4})	4.2×10^3 (1.2×10^4)	7.1 (7.1)	10.9 (0.003)	1435 (0.77)	1.9 (1.9×10^{-7})

of the tube. In these layers, $\beta < 1$ inside the flux tube as shown in Fig 1.

Wave excitation is carried out by implementing velocity drivers at the bottom boundary. We use a horizontal driver to mimic the granular buffeting motion and a torsional driver to mimic the effect of vortex-like motion. The driving motions at the bottom boundary are specified using the following velocity drivers.

$$V_x(x,y,0,t) = \begin{cases} V_0 \sin(2\pi t/P) & \text{for} \quad 0 \leq t \leq P/2\,, \\ 0 & \text{for} \quad 0 > t > P/2\,. \end{cases} \quad \text{(Horizontal)} \qquad (1)$$

$$V_\phi(x,y,0,t) = \begin{cases} -V_0 \tanh\left(\frac{2\pi r}{\delta r}\right) \sin\left(\frac{2\pi t}{P}\right) & 0 \leq t \leq P/2\,, \\ 0 & t > P/2\,. \end{cases} \quad \text{(Torsional)} \qquad (2)$$

These driving motions generate slow (predominantly acoustic) and fast (predominantly magnetic) waves in the model along with the intermediate Alfvén wave which we do not consider in this study.
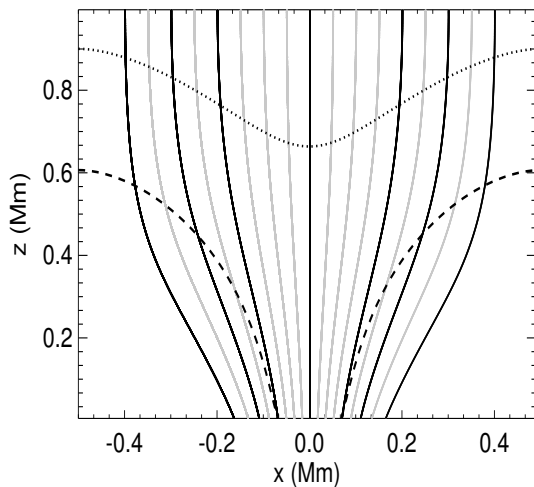
Figure 1. Two-dimensional representation of the flux-tube model. The solid lines mark the magnetic field lines on a x-z plane at $y = 0$ Mm. The $\beta = 1$ (- - - -) and $\beta = 0.1$ ($\cdots\cdots$) contours are also shown.

3. Numerical Simulation

The three-dimensional numerical simulations were carried out using the Sheffield Advanced Code [13]. The code uses a modified version of the set of MHD equations to deal with a strongly stratified magnetized medium. In this study, we solve the full set of ideal magnetohydrodynamic equations in three dimensions to study the propagation of waves in the computational domain. The domain is a 1 Mm $\times$ 1 Mm $\times$ 1 Mm cube discretized on $100 \times 100 \times 100$ grid points. We use transmitting boundary conditions at the top and side boundaries to allow the waves to propagate out of the simulation box.

The simulation starts with a localized, time dependent perturbation at the bottom boundary resulting in the excitation of various kinds of MHD modes with different strength. The gas pressure perturbations drive slow magneto-acoustic wave (SMAW) within the $\beta < 1$ region and fast magneto-acoustic wave (FMAW) in the ambient medium where $\beta > 1$. The magneto-acoustic wave propagation can be seen in the velocity and temperature perturbation in the medium as shown in Fig 2. We notice that the horizontal excitation generates strong SMAW within the flux tube as can be seen in the temperature fluctuations. Since the SMAW propagates along field lines, we also see strong velocity parallel to the field lines. The torsional excitation on the other hand generates SMAW that are weaker than those generated by the horizontal driver. In the previous study [12], we estimated the energy transport by MHD waves for the two driving cases. The energy fluxes were calculated on a representative field line and we showed that there is a strong acoustic flux associated with SMAW in the case of the horizontal excitation, which is two orders of magnitude more than that for the case of torsional excitation. However, these studies were restricted to a single field line and hence it was not possible to assess the response of the whole flux tube to the different perturbations that were considered. In this paper, we extend the previous study by looking at the flux tube as a whole and estimating the total acoustic emission from various physical surfaces relevant to the model. Due to the nature of the drivers, the analysis on a single field line depends wholly on the location of the footpoint of the chosen field line with respect to the driving motion. Especially, in the case of a horizontal motion, where the strongest perturbations is localized to a small region on either side of the $y = 0$ plane. Also, since the velocity driver acts in region where $\beta < 1$ (close to the axis) as well as $\beta > 1$ (outer regions), a field line located in either of these region sees a different mode of magneto-acoustic wave. Considering an ensemble of field lines will give a better idea about the reaction of the flux tube as a whole to the excitation at the base.
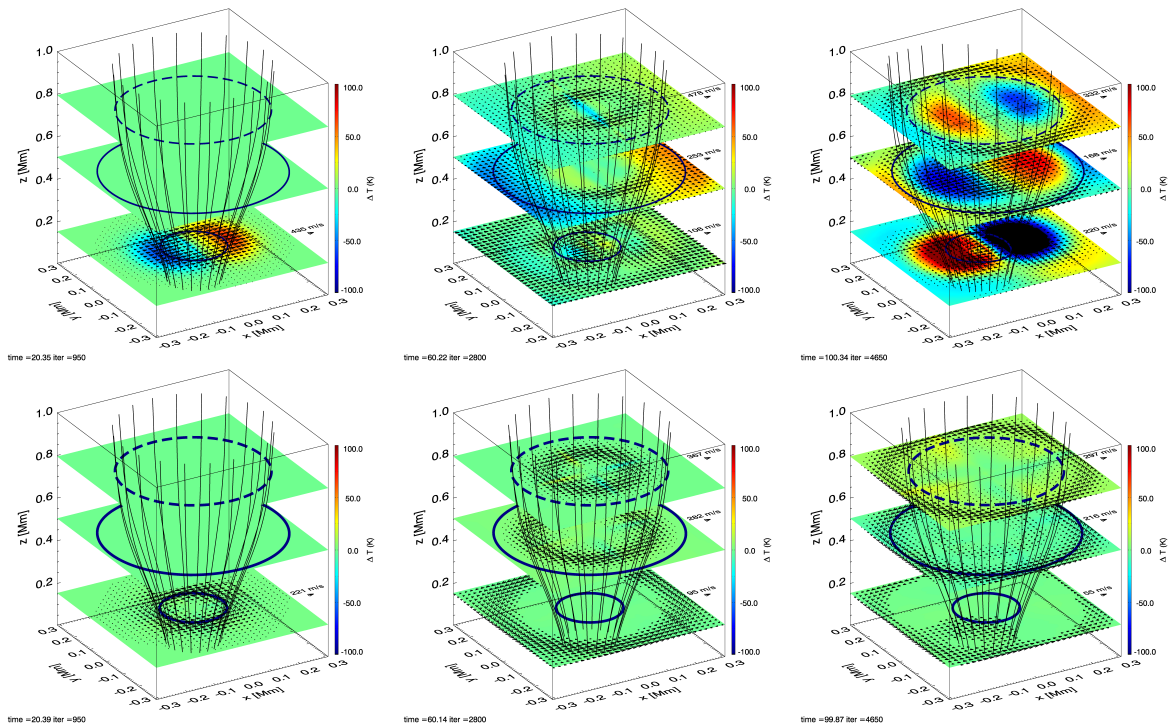
Figure 2. *Top:* Temperature perturbations at t=20 s,60 s, and 100 s at different heights as a result of a transversal uni-directional excitation. *Bottom*: Temperature fluctuations as a result of torsional excitation. The projected velocity vectors on the *x-y* plane are shown at each height. The thick blue curve depicts the $\beta=1$ region and the blue dashed curve shows the $\beta=0.1$ region.

4. Results

4.1. Longitudinal & Lateral emission

Apart from acting as a conduit for MHD waves to the overlying layers, the perturbed flux tube also transfers energy to the ambient medium in the form of acoustic waves. It is interesting to look at acoustic energy flux leaking out of the flux tube boundary and how it depends on the nature of the excitation that the flux tube undergoes. Since we consider here a thick flux tube, a strict definition of the flux tube boundary is ambiguous. However, for the purpose of this study, we choose the surfaces of equal magnetic potential or the magnetic isosurface as representative levels in the flux tube for purposes of calculating the fluxes. The cross-section of the magnetic isosurface at any given height is a circle centered at the axis, due to the cylindrical symmetry of the initial model. This allows us to define a circle at a radial distance r of the flux tube on any horizontal plane. We calculate the acoustic flux on three magnetic isosurfaces crossing radial distance of $r = 0.2$ Mm, 0.3 Mm and 0.4 Mm from the axis of the flux tube at $z = 1$ Mm. The magnetic field lines that define this isosurface can be identified from the equilibrium model and they remain the same throughout the simulation, allowing us to calculate physical quantities on this surface as it evolves. The velocity vector at any point on this surface can be decomposed into three orthogonal components, *viz.* parallel (v_s), normal (v_n) and azimuthal (v_ϕ) component. The calculation of these component for a single field line is described in [12]. Using these velocity components for a collection of field lines defining various isosurfaces, we calculate the parallel and normal acoustic fluxes according to,

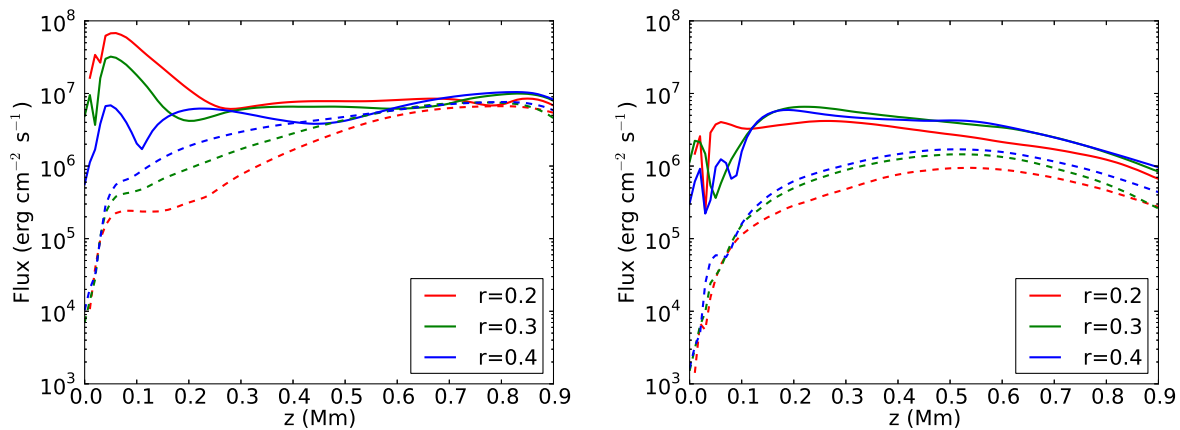$$F_{s,n} = \Delta p v_{s,n} \qquad (3)$$

Figure 3. *Left*: Time-averaged longitudinal acoustic flux on the three isosurfaces for the horizontal (Solid lines) and torsional(dashed lines) excitation cases. *Right* Normal acoustic flux on the three isosurfaces.

where Δp is the gas pressure perturbation from the equilibrium. Acoustic fluxes are calculated on field lines corresponding to three magnetic isosurfaces. In Figure 3, the left panel shows the time averaged parallel acoustic fluxes (F_s) on field lines associated with different isosurfaces as a function of height. The horizontal excitation results in relatively stronger acoustic emission compared to torsional excitation in the lower part of the flux tube. But, the averaged fluxes tend to be similar as we go higher up in the atmosphere, since in the horizontal excitation case, only a small fraction of field lines on either side of the tube partake in transporting the longitudinal fluxes. The right panel of Fig. 3 shows the time averaged acoustic flux directed normal to the flux-tube boundaries, which is significantly lower than the fluxes directed along the field lines in the tube.

4.2. β-surface emission

The surface of equipartition ($\beta=1$ layer) between thermal and magnetic energy density influences the MHD modes by acting as region of wave transmission and conversion. As a preliminary step towards understanding this region more closely, we look at the acoustic energy flux crossing normal to the surfaces of constant plasma β surface (β isosurfaces). In this study, we mainly focus on the $\beta = 1$ isosurface, since this is where the different MHD modes undergo strong coupling which eventually leads to the generation of Alfvén waves in the upper chromosphere. The whole process proceeds in two stages. Initially, the magneto-acoustic modes encounter the equipartition zone as they propagate to the upper layers of the atmosphere. The energy in the modes get redistributed partially by transmission and partially by conversion to other modes. The transmission and conversion depends on the properties of the wave and the background magnetic field across this zone of influence [14]. In the second stage, the mode converted magnetic wave (FMAW) propagates up to a certain height after which it gets partially reflected down and partially gets converted to Alfvén waves due to steep gradients in the Alfvén speed [15]. A better understanding of the energy distribution during the initial stage where mode coupling occurs across the $\beta = 1$ surface is nessasary to further evaluate the energy available for Alfvén wave. To this end, we look at the acoustic flux directed normal to the surface of $\beta = 1$ and compare it with that from a $\beta = 0.1$ isosorface which lies well above in the atmosphere. It should be noted that in the lower part of the flux tube, the $\beta = 1$ surface normal points towards the axis of the flux-tube.
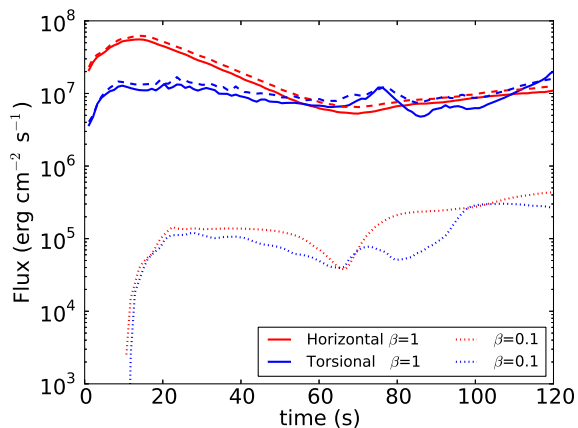
Figure 4. Time evolution of the normal acoustic flux on $\beta{=}1$ (solid line) and $\beta{=}0.1$ (dotted) surface for horizontal (red line) and torsional (blue) excitation of a magnetic flux tube

Figure 4 shows the spatially averaged acoustic flux directed normal to the surfaces of constant β for $\beta{=}1$ and 0.1 as a function of time. We clearly see that the acoustic emission from the $\beta{=}1$ surface is stronger compared to the emission on the $\beta{=}0.1$ surface for both horizontal and torsional excitations. The $\beta{=}1$ surface responds more efficiently to a horizontal uni-directional motion at the foot-point by emitting more acoustic flux normal to the surface. Our analysis is limited by the fact that we consider a strong flux tube where the $\beta = 1$ surface dips below the bottom boundary near the axis of the flux tube. To have a better understanding about this layer, we need to look at flux tubes models with $\beta = 1$ surfaces at different levels in the atmosphere.

5. Summary & Conclusions

Three dimensional numerical simulation of wave propagation in a magnetic flux tube embedded in a solar atmosphere were carried out. We investigated two types of excitation mechanism, viz. transversal and torsional, that are characteristic processes by which waves can be generated in the real solar atmosphere. We calculated the acoustic energy components at various levels in the flux tube as well as on the surfaces defined by constant plasma β of the flux tube due to the driving footpoint motions. We observe that the acoustic power is predominantly directed vertically upward along the flux tube in both cases. The lateral acoustic emission from the boundary of the flux tube in both cases of horizontal and torsional excitations is much lower. The magnetic flux tube acts as an efficient conduit for acoustic waves, with negligible acoustic leakage from the tube boundary. Most of the acoustic energy produced due to photospheric disturbances are efficiently transported and are made available to higher layers regardless of the source of the disturbance. As far as the comparison between the two excitation scenarios in terms of acoustic energy transport to upper layers is concerned, we have not been able to conclusively point out which of the two mechanisms is more efficient. This is partly due to the axisymmetric equilibrium model that we have used and the idealistic driving mechanisms that we consider in the study. Nevertheless, our analysis supports that the magnetic field mediates the coupling between various photospheric disturbances and the upper layers. However meagre their contribution to the overall energy output is, these scenarios must be considered when evaluating the available energy sources for the heating of chromosphere and corona. The surface of equipartition between magnetic and thermal energy density ($\beta = 1$) is a strong source of acoustic emission in both excitation scenarios and would be the focus of future investigations.

References

[1] de Wijn A G, Stenflo J O, Solanki S K and Tsuneta S 2009 *Space Sci. Rev.* **144** 275–315
[2] Jess D B, Mathioudakis M, Erdélyi R, Crockett P J, Keenan F P and Christian D J 2009 *Science* **323** 1582–1585
[3] Hasan S S and van Ballegooijen A A 2008 *Astrophys. J.* **680** 1542–1552
[4] van Ballegooijen A A, Asgari-Targhi M, Cranmer S R and DeLuca E E 2011 *Astrophys. J.* **736**
[5] Kato Y, Steiner O, Steffen M and Suematsu Y 2011 *Astrophys. J. Lett.* **730** L24
[6] Wedemeyer-Böhm S, Scullion E, Steiner O, Rouppe van der Voort L, de La Cruz Rodriguez J, Fedun V and Erdélyi R 2012 *Nature* **486** 505–508
[7] Hasan S S, van Ballegooijen A A, Kalkofen W and Steiner O 2005 *Astrophys. J.* **631** 1270–1280
[8] Khomenko E, Collados M and Felipe T 2008 *Sol. Phys.* **251** 589–611
[9] Vigeesh G, Hasan S S and Steiner O 2009 *Astron. Astrophys.* **508** 951–962
[10] Kitiashvili I N, Kosovichev A G, Mansour N N and Wray A A 2011 *Astrophys. J. Lett.* **727**
[11] Fedun V, Verth G, Jess D B and Erdélyi R 2011 *Astrophys. J. Lett.* **740** L46
[12] Vigeesh G, Fedun V, Hasan S S and Erdélyi R 2012 *Astrophys. J.* **755** 18
[13] Shelyag S, Fedun V and Erdélyi R 2008 *Astron. Astrophys.* **486** 655–662
[14] Cally P S 2007 *Astron. Nachr.* **328** 286
[15] Khomenko E and Cally P S 2012 *Astrophys. J.* **746** 68